

## UNDERWATER MAPPING FROM AERIAL PHOTOGRAPHY

Dr. Wheda M.S.  
Al-Fatah University  
P.O.Box 81235 Tripoli  
Libya

### ABSTRACT

The need for an accurate and less expensive underwater mapping system has long been, and still is, very important. Many agencies within governments are interested in mapping underwater features for different reasons. Maps are needed for coastal engineering, geological and mineral explorations, army amphibious operations, ship navigations, etc. This paper is a part of a research that investigates the possibility of producing hydrographic maps of visible underwater shore bottoms using analytical photogrammetry. It utilizes multiple overlapping aerial photos in a simultaneous solution, whereas present photogrammetric methods use only stereopairs, and are thus subject to very significant errors due to unpredictable water-air interfaces caused by surface waves. In this system the redundancy produced compensates for these errors to a very significant degree.

In this research a mathematical model was developed to account for refraction at the water surface, and solve for most probable position of underwater features directly. The model was tested using photographs of underwater targets in a water channel taken with a 70 mm non-metric camera in a laboratory environment. It was also tested using archived photographs. The results obtained using multi-overlapped photographs showed greater accuracy improvement compared with using only one stereopair.

### INTRODUCTION

When underwater features are photographed from the air, light rays reflected or emitted from underwater objects undergo some refraction when passing through one medium to another, i.e., water to air. Different light rays bend at the air water interface in different directions and by different amounts. The amount and direction of refraction is highly dependent on the two-media properties and the interface roughness.

According to a Snell's Law of Refraction, the amount of refraction is a function of the angle of incidence and Index of Refraction. If the interface is flat and level, the normal coincides with the vertical "direction of gravity." However, this is rarely the case since there are usually surface waves which complicate the situation a great deal.

In effect, this paper is part of a research that seeks to fully define the problems involved with using aerial photographs in underwater mapping, and to develop analytical system that minimizes the errors involved and improves the accuracy attained.

## MECHANICAL MODEL

The mathematical development contained is based on the following assumptions:

- the camera exterior and interior orientation parameters are assumed to be known for every camera station.
- the water index of refraction is known and constant.
- the wave system at the air-water interface is sinusoidal; its parameters (wave length, wave amplitude, and wave direction) are assumed to be known.

To help understand the mathematics involved the mode is divided to the following steps.

1. Develops the necessary equations to determine where light rays reflected from underwater objects intersect the water surface.

Assuming that the horizontal datum is the mean local surface of a water body at the time of photography, the collinearity equations are:

$$x_i = -f \left[ \frac{m_{11}(X_i - X_L) + m_{12}(Y_i - Y_L) + m_{13}(Z_i - Z_L)}{m_{31}(X_i - X_L) + m_{32}(Y_i - Y_L) + m_{33}(Z_i - Z_L)} \right] \dots(1)$$

$$y_i = -f \left[ \frac{m_{21}(X_i - X_L) + m_{22}(Y_i - Y_L) + m_{23}(Z_i - Z_L)}{m_{31}(X_i - X_L) + m_{32}(Y_i - Y_L) + m_{33}(Z_i - Z_L)} \right] \dots(2)$$

where:

$x_i, y_i$  = refined image coordinates of ground point  $i$

$f$  = the camera focal length

$X_i, Y_i, Z_i$  = ground coordinates of point  $i$

$X_L, Y_L, Z_L$  = ground coordinates of the exposure station

and  $m_{ij}$  = are rotation matrix coefficients.

Substituting  $-H$  for  $Z_i - Z_L$  in equations (1) and (2) and rearranging,  $X_i$  and  $Y_i$  coordinates at the local datum can be determined as follows:

$$X_i = X_L + H \frac{x_i(m_{23}m_{32} - m_{33}m_{22}) + y_i(m_{33}m_{12} - m_{32}m_{12}) + f(m_{23}m_{12} - m_{13}m_{22})}{x_i(m_{32}m_{21} - m_{31}m_{22}) + y_i(m_{12}m_{31} - m_{11}m_{32}) + f(m_{12}m_{21} - m_{11}m_{22})} \quad (3)$$

$$Y_i = Y_L + H \frac{x_i(m_{23}m_{31} - m_{21}m_{33}) + y_i(m_{33}m_{11} - m_{31}m_{13}) + f(m_{23}m_{11} - m_{21}m_{13})}{x_i(m_{22}m_{31} - m_{21}m_{32}) + y_i(m_{32}m_{11} - m_{31}m_{12}) + f(m_{22}m_{11} - m_{21}m_{12})} \quad (4)$$

Using equations (3) and (4) (i.e., the reordered collinearity equations), the known parameters of the camera station, and the image coordinates, X and Y coordinates of point i at the water mean level can be determined.

## 2. Determining Where Light Rays Intersect the Water Surface.

Using refined image coordinates and camera station exterior orientation parameters, the X, Y and Z coordinates of points where light rays coming from an underwater object, intersect with the wave surface can be located. After reordering the photogrammetric collinearity equations, they can then be used to determine imaginary points at the mean water surface level from each pair of image coordinates. These points and the wave system equations are used to iteratively determine where light rays intersect the water surface.

## 3. Determining Incident and Refracted Angles.

The incident angle  $\theta$  between the normal at a point and the light ray above water, and refracted angle  $r$  between the normal and the light ray underwater, can be calculated as follows:

$$\theta = \cos^{-1}(\cos\beta \sin\xi \sin\delta + \cos\gamma \sin\xi \cos\delta + \cos\mu \cos\xi) \dots (5)$$

$$r = \sin^{-1}\left[\frac{\sin\theta}{n}\right] \dots \dots \dots (6)$$

Where:

- $\xi$  = Slope of the wave
- $\delta$  = The azimuth of the normal to the wave surface
- $\beta$  = The angle that the light ray makes with x-axis
- $\gamma$  = The angle that the light ray makes with y-axis
- $\mu$  = The angle that the light ray makes with z-axis

## 4. Observation Equations and Least Squares Algorithm.

Each pair of image coordinates generates two equations. Two photos provide four observation equations, or one degree of freedom. Thus, the more photographs that image the underwater features from different locations, the better the final determination of spatial coordinates of underwater features. Equations in the form of observation equations can be written in terms of angles that underwater light rays make with the vertical, and that the azimuths make with ground north.

$$\theta_{m_i} + v_{\theta_i} = \tan^{-1} \left[ \frac{(X-X_A)^2 + (Y-Y_A)^2}{(Z_L - Z_S - h)^2} \right]^{1/2} \dots \dots (7)$$

$$\alpha_{m_i} + v_{\alpha_{m_i}} = \tan^{-1} \left( \frac{X-X_A}{Y-Y_A} \right) \dots \dots \dots (8)$$

Equations (7-8) are non linear, but can be linearized using Taylor Series. First the function are rewritten as:

$$\text{Let } F = 0 = \tan^{-1} \left[ \frac{(X-X_A)^2 + (Y-Y_A)^2}{(Z_L - Z_S - h)^2} \right]^{1/2} - \theta_{m_i} - v_{\theta_i}$$

$$\text{Let } G = \tan^{-1} \left( \frac{X-X_A}{Y-Y_A} \right) - \alpha_{m_i} - v_{\alpha}$$

Then according to Taylor's Theorem,

$$F = (F)_0 + \left( \frac{\partial F}{\partial X} \right)_0 dX + \left( \frac{\partial F}{\partial Y} \right)_0 dY + \left( \frac{\partial F}{\partial h} \right)_0 dh$$

$$G = (G)_0 + \left( \frac{\partial G}{\partial X} \right)_0 dx + \left( \frac{\partial G}{\partial Y} \right)_0 dy + \left( \frac{\partial G}{\partial h} \right)_0 dh$$

where:

$$\frac{\partial F}{\partial X} = \frac{(X-X_A)(Z_L - Z_S - h)}{[(Z_L - Z_S - h)^2 + (X-X_A)^2 + (Y-Y_A)^2] [(X-X_A)^2 + (Y-Y_A)^2]^{1/2}}$$

$$\frac{\partial F}{\partial Y} = \frac{(Y-Y_A)(Z_L - Z_S - h)}{[(Z_L - Z_S - h)^2 + (X-X_A)^2 + (Y-Y_A)^2] [(X-X_A)^2 + (Y-Y_A)^2]^{1/2}}$$

$$\frac{\partial F}{\partial h} = \frac{-[(X-X_A)(Y-Y_A)]^2}{[(Z_L - Z_S - h)^2 + (X-X_A)^2 + (Y-Y_A)^2]}$$

$$\frac{\partial G}{\partial X} = \frac{(Y-Y_A)}{[(X-X_A)^2 + (Y-Y_A)^2]}$$

$$\frac{\partial G}{\partial Y} = \frac{(X-X_A)}{[(X-X_A)^2 + (Y-Y_A)^2]}$$

$$\frac{\partial G}{\partial h} = 0.$$

A least squares solution is performed for every point. The first two rows of the observation matrix become as follows:

$$\begin{array}{ll} A(1,1) = \partial F / \partial X & A(2,1) = \partial G / \partial X \\ A(1,2) = \partial F / \partial Y & A(2,2) = \partial G / \partial Y \\ A(1,3) = \partial F / \partial h & A(2,3) = 0. \end{array}$$

#### RESULTS FROM LAB EXPERIMENT

The horizontal X, Y coordinates of underwater targets in the lab experiment were accurately determined. When nine overlapped photos were used, these horizontal positions were precisely calculated, regardless of the water surface conditions. But when only two photos were used horizontal accuracy decreased as surface roughness increased.

It can be concluded that use of nine photos, rather than two, when waves are present decreases the error in depth (Z) by a factor of from 4 to 10, depending on the depths of targets. If four photos instead of nine are used the increase in accuracy would still be significant but not as dramatic. Here, the errors are reduced by factors of from 2 to 5.

#### FIELD TEST USING ARCHIVAL PHOTOGRAPHS

Photo coordinates of nineteen points (23-41) see Fig. 1 were measured on three overlapped photos taken from the archives of the Surveyor General of Western Australia over 'Rottnest' an island on the western shore of Australia. These points were used to test the mathematical model developed earlier. Depths of underwater points resulting from the adjustment were compared with depths interpolated from existing hydrographic charts established by sounding techniques. Table 1 summarizes this comparison. The accuracy of sounding depths was not established but, it is reasonable to assume a value of 0.5 meters applies. The resultant differences in this table can be considered reasonably accurate.

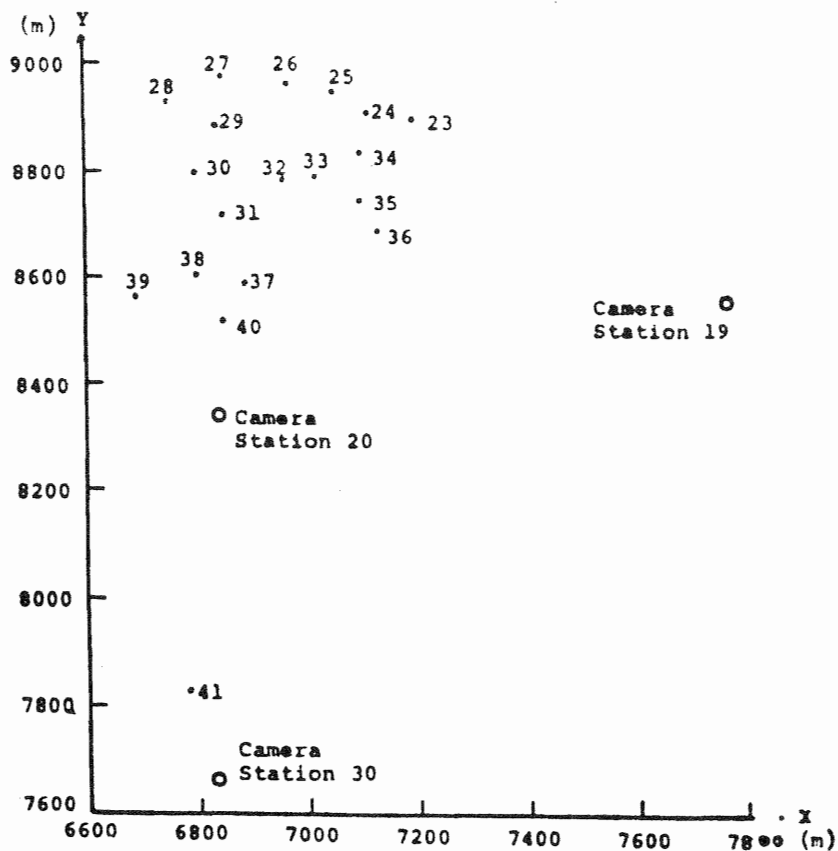


Fig.1. Location of underwater points (23-41) with respect to camera stations. Coordinates are in meters.

Table 1 Field test results from archive photographs (units are in meters).

point #	calculated depth	interpolated depth	difference
23	-6.233	-5.94	+.29
24	-7.045	-7.04	+.00
25	-8.232	-8.94	-.71
26	-9.414	-10.64	-1.23
27	-12.170	-12.44	-.17
28	-12.856	-13.34	-.48
29	-11.185	-12.04	-.86
30	-11.132	-11.94	-.81
31	-10.207	-10.84	-.63
32	-7.962	-8.94	-.98
33	-6.819	-7.24	-.42
34	-6.418	-6.64	-.22
35	-5.335	-5.34	+.00
36	-5.833	-6.94	-1.11
37	-8.079	-8.84	-.76
38	-10.494	-11.14	-.65
39	-14.928	-12.14	+1.79
40	-7.101	-7.94	-.84
41	-4.321	-2.44	+1.98

Calculated depths: calculated photogrammetrically

Interpolated depths: interpolated from hydrographic charts

## CONCLUSIONS

Despite the fact that this test was forced to rely on three photographs, which provided only three degrees of freedom rather than up to fifteen degrees of freedom (the result if nine photos were used), calculation of underwater positions was reasonably accurate. (More ideal situations can, of course, be pre-planned.) Also, considering that the location of these underwater points did not involve the best photogrammetric geometry (such that almost all points were on one side of the flight lines, as shown in Fig. 1), this test was nonetheless successful. However, in future studies, geometry could be improved both by having 60-70% side and forward overlaps, and by using only the center areas, where underwater points would appear on at least four photos and possibly as many as nine.

## REFERENCES

- American Society of Photogrammetry, Manual of Photogrammetry, Fourth Edition, Falls Church, Va. 1980.  
Wheda Massoud S., Ph.D. thesis, University of Wisconsin-Madison 1985.  
Wolf Paul R., Elements of Photogrammetry, McGraw-Hill Book Co., New York, 1983.

## ACKNOWLEDGEMENT

I would like to express my sincere thanks to professor James Scherz who contributed a great deal to this research, Mr. W.G. Henderson and Mr. Ray Webster, for their help with the field test data.